© 2023. Published by The Company of Biologists Ltd | Journal of Experimental Biology (2023) 226, jeb246304. doi:10.1242/jeb.246304

RESEARCH ARTICLE

Physiological responses to acute warming at the agitation temperature in a temperate shark

Ian A. Bouyoucos[1,2,*], Alyssa M. Weinrauch[1,2], Ken M. Jeffries[1] and W. Gary Anderson[1,2]

ABSTRACT

Thermal tolerance and associated mechanisms are often tested via the critical thermal maximum (CT_{max}). The agitation temperature is a recently described thermal limit in fishes that has received little mechanistic evaluation. The present study used a temperate elasmobranch fish to test the hypothesis that this thermal tolerance trait is partially set by the onset of declining cardiorespiratory performance and the cellular stress response. Pacific spiny dogfish (*Squalus suckleyi*) were screened for cardiorespiratory and whole-organism thermal limits to test for associations between thermal performance and tolerance. Then, biochemical markers of secondary stress, aerobic and anaerobic enzyme activities, and molecular markers of cellular stress were determined for various tissues at the agitation temperature and secondary stress markers were determined at CT_{max}. In dogfish, the agitation temperature was characterised by increased turning activity within experimental chambers and was equal to the temperature at which dogfish exhibited maximum heart rate. Citrate synthase activity increased at the agitation temperature in white muscle relative to unmanipulated dogfish. Furthermore, lactate dehydrogenase activity and accumulated lactate in the plasma and muscle were not affected by acute warming. Cellular stress was apparent in hypothalamus, gill filament and ventricle, denoted by elevated transcript abundance of the stress response gene *hsp70* but not the oxygen homeostasis gene *hif1α*. Conversely, CT_{max} was characterised by metabolic acidosis driven by anaerobic lactate production, signifying an increased reliance on anaerobic metabolism between the agitation temperature and CT_{max}. Together, these data provide partial support for our hypothesis, in that cellular stress, but not declining thermal performance, occurred at the agitation temperature.

KEY WORDS: Critical thermal maximum, Elasmobranch fish, Heart rate, Heat shock protein, Hypoxia-inducible factor, Thermal tolerance

INTRODUCTION

Acute changes in ambient environmental temperatures can limit the performance of physiological systems. In aquatic environments, body temperatures of poikilothermic ectotherms, such as fishes and invertebrates, closely match prevailing environmental temperatures. Thus, rapidly increasing temperatures can lead to changes in whole-organismal performance through direct thermal effects on molecular and biochemical processes (Little et al., 2020; Schulte et al., 2011). Putative mechanisms of upper thermal tolerance limits in aquatic ectotherms have largely focused on thermal limits of key organs or organelles of critical physiological systems. For instance, thermal limits of cardiorespiratory system performance, examined via heart and mitochondrial function (Anttila et al., 2013; Chung and Schulte, 2020), or nervous system performance, examined via brain and ion channel function (Andreassen et al., 2022; Haverinen and Vornanen, 2020), underscore various hypotheses pertaining to whole-organism thermal limits. Indeed, at the whole-organism level, thermal tolerance is a complex phenomenon with no single defining mechanism (Ern et al., 2023; MacMillan, 2019). Furthermore, numerous thermal tolerance metrics have been proposed in aquatic ectotherms (Desforges et al., 2023), and each metric is possibly set by different mechanisms.

Among the most measured upper thermal tolerance metrics is the critical thermal maximum (CT_{max}). Experimentally, CT_{max} is defined for fishes exposed to acute warming at a constant rate as the temperature when neuromotor control becomes disorganized, often realized as an inability to maintain upright orientation (Becker and Genoway, 1979; Lutterschmidt and Hutchison, 1997). As such, CT_{max} is often interpreted as 'ecological death', where a fish exposed to its CT_{max} in the wild would not be able to function in an ecologically meaningful capacity (Beitinger et al., 2000). Several studies have demonstrated that experimentally derived CT_{max} estimates can closely approximate upper thermal limits to the distribution of some fish populations (Jeffries et al., 2016; Payne et al., 2021); however, methods to estimate CT_{max} are often inconsistent across studies (i.e. heating rate and behavioural endpoint) and the ecological relevance of CT_{max} is questioned (Desforges et al., 2023). In addition, underlying mechanisms of CT_{max} are equivocal, or, at least, non-universal (Ern et al., 2023). For example, oxygen limitation is an oft-tested mechanism of upper thermal tolerance in fishes and aquatic invertebrates (McArley et al., 2022), and findings suggest that aquatic ectotherms express either oxygen-dependent or oxygen-independent upper thermal tolerance phenotypes (Ern et al., 2016, 2020). Brain dysfunction has also been proposed as a mechanism underlying CT_{max} (Andreassen et al., 2022; Jutfelt et al., 2019). There is also interest in comparing alternative thermal tolerance traits, such as CT_{swim} (Blasco et al., 2020), shifts at the transcriptional level (Jeffries et al., 2018) or the agitation temperature (McDonnell and Chapman, 2015) to CT_{max}.

The agitation temperature is a novel upper thermal tolerance metric in fishes. It is well described that ectotherms increase their activity with acute warming in an attempt to escape until a CT_{max} endpoint is reached (Lutterschmidt and Hutchison, 1997). This escape behaviour was first used to define a thermal tolerance endpoint by McDonnell and Chapman (2015), who noted that the African cichlid (*Pseudocrenilabrus multicolor victoriae*) would leave shelter and increase swimming activity in an agitated manner during measurement of CT_{max}, presumably seeking more

[1]Department of Biological Sciences, University of Manitoba, Winnipeg, MB, Canada, R3T 2N2. [2]Bamfield Marine Sciences Centre, Bamfield, BC, Canada, V0R 1B0.

*Author for correspondence (ian.bouyoucos@umanitoba.ca)

I.A.B., 0000-0002-4267-1043; A.M.W., 0000-0001-5710-0035; K.M.J., 0000-0002-7466-1915; W.G.A., 0000-0002-0427-8216

Received 14 June 2023; Accepted 4 September 2023

Journal of Experimental Biology (2023) 226, jeb246304. doi:10.1242/jeb.246304

List of symbols and abbreviations

CS	citrate synthase
CT_{max}	critical thermal maximum
f_H	heart rate
f_V	ventilation rate
$[K^+]$	plasma potassium concentration
LDH	lactate dehydrogenase
pH_i	intracellular pH
Q_{10}	temperature coefficient
T_{AB}	Arrhenius breakpoint temperature
T_{peak}	temperature of peak heart rate

favourable, cooler waters. As such, the agitation temperature is interpreted as a behavioural response to thermal stress. Since this study, numerous others have quantified the agitation temperature and demonstrated that it occurs before CT_{max} (Enders and Durhack, 2022; Kochhann et al., 2021; Turko et al., 2020; Wells et al., 2016) and is responsive to temperature acclimation and acute hypoxia (Firth et al., 2021; McDonnell et al., 2019, 2021; Potts et al., 2021). Because the agitation has been shown to be sensitive to acute hypoxia, studies have suggested that cardiorespiratory performance may set the agitation temperature (McDonnell et al., 2021; Potts et al., 2021). In particular, McDonnell et al. (2021) demonstrated that the agitation temperature, and not CT_{max}, was affected by acclimation to hypoxic conditions, and suggested that this apparent uncoupling of physiological and behavioural thermal thresholds implies different mechanisms affecting either trait. Notably, there is a lack of a mechanistic understanding of the physiology at the onset of agitation behaviour at temperatures nearing CT_{max}.

Thermal tolerance mechanisms in elasmobranch fishes are poorly understood. To date, eight studies have quantified CT_{max} in seven species of elasmobranch fishes: (i) four tropical species: the epaulette shark (*Hemiscyllium ocellatum*; Gervais et al., 2018; Wheeler et al., 2022), ribbontail stingray (*Taeniura lymma*; Dabruzzi et al., 2013), blacktip reef shark (*Carcharhinus melanopterus*; Bouyoucos et al., 2020, 2021) and sicklefin lemon shark (*Negaprion acutidens*; Bouyoucos et al., 2021); and (ii) three temperate species: the Atlantic stingray (*Hypanus sabinus*; Fangue and Bennett, 2003), Port Jackson shark (*Heterodontus portusjacksoni*; Gervais et al., 2021) and chain catshark (*Scyliorhinus rotifer*; Lupton and Bennett, 2023). These studies predominantly tested for effects of temperature acclimation on CT_{max} without testing underlying mechanisms. Studies in *C. melanopterus* and *N. acutidens* demonstrated correlations between CT_{max} and various traits relating to oxygen supply capacity (e.g. hypoxia tolerance, haematocrit), but did not directly test for oxygen-limitation of thermal tolerance (Bouyoucos et al., 2020, 2021). A putative mechanism of thermal tolerance has also been proposed that is unique to elasmobranch fishes. Comparatively high concentrations of the chemical chaperone, trimethylamine oxide (TMAO), found in the tissues and plasma of elasmobranch fishes serve similar roles as heat shock proteins (Villalobos and Renfro, 2007). However, conflicting reports of the responsiveness of TMAO and heat shock proteins to acute thermal stress have been published (Bockus et al., 2020; Kolhatkar et al., 2014).

The purpose of this study was to test physiological responses to warming at the agitation temperature using a temperate elasmobranch fish, the Pacific spiny dogfish (*Squalus suckleyi*). Specifically, this study's overarching hypothesis was that whole-organism thermal tolerance traits (i.e. the agitation temperature) are partially set by cardiorespiratory thermal limits and thermal stress. The first study objective was to define a suite of sub-lethal upper thermal limits using behavioural proxies and cardiorespiratory limits. We predicted that cardiorespiratory thermal limits would occur at lower temperatures than whole-organism thermal tolerance limits (i.e. the agitation temperature and CT_{max}). The second study objective was to quantify biochemical markers of secondary stress occurring in the plasma at CT_{max}. We predicted that fish would exhibit signs of metabolic acidosis, such as depressed intracellular pH and plasma lactate accumulation. The third study objective was to measure plasma and muscle lactate concentrations, activities of aerobic and anaerobic enzymes, and mRNA transcript abundance of temperature and hypoxia stress genes at the agitation temperature. We predicted that various tissues would accumulate lactate, demonstrate increased activity of anaerobic (i.e. lactate dehydrogenase) and aerobic enzymes (i.e. citrate synthase), and increase abundance of stress-responsive mRNA transcripts (i.e. *hsp70*, *hif1α*). Together, the present study provides new data on putative physiological mechanisms underpinning the agitation temperature and expands knowledge on thermal tolerance in elasmobranch fishes.

MATERIALS AND METHODS

Ethical approvals

Male spiny dogfish (*Squalus suckleyi* Girard 1855) were collected under Fisheries and Oceans Canada permit XR-199 2022. Female dogfish were not collected because female dogfish are known to be gravid during the study period (Tribuzio and Kruse, 2012). Experiments were approved by the Bamfield Marine Sciences Centre (BMSC) Animal Care Committee (animal user protocol RS-22-10).

Animal collection and husbandry

Male spiny dogfish were captured using rod and reel, and demersal longline in Barkley Sound (Bamfield, British Columbia, Canada) during July and August 2022. Dogfish were transported to BMSC where they were maintained in a 155,000 liter tank. The holding tank was continuously supplied with seawater (11°C, 32 ppt) and dogfish were fed cut hake (*Merluccius productus*) every 4 days, *ad libitum*. Prior to experimentation, dogfish were fasted for at least 72 h. After experimentation, all individuals were euthanized with emersion in an overdose of tricaine methanesulfonate (MS-222; >0.2 g l^{-1}) followed by cervical dislocation.

Objective 1: thermal tolerance limits

Thermal tolerance limits were defined using whole-organism and cardiorespiratory endpoints. Whole-organism endpoints representing thermal tolerance were the CT_{max} (the temperature denoting the onset of muscle spasms; Bouyoucos et al., 2020) and agitation temperature (denoting the temperature where fish exhibit avoidance behaviour of warming water; McDonnell and Chapman, 2015). Cardiorespiratory endpoints representing thermal tolerance were the Arrhenius breakpoint temperature (T_{AB}; Casselman et al., 2012) and temperature of peak heart rate (T_{peak}; Gilbert et al., 2020). Seven dogfish (mass=2.25±0.42 kg; data are presented as means±s.d. unless otherwise noted) were screened for all thermal tolerance endpoints.

Whole-organism thermal tolerance endpoints

Dogfish were rapidly transported by hand from their holding tank to acrylic boxes (90×30×15 cm). Boxes were partially submerged in a

173 l trough (170×73×14 cm). The water level within boxes was 14 cm, which was enough to fully submerge dogfish. Each box was connected to a 300 l h^{-1} pump (Eheim GmbH & Co., Deizisau, Germany) to circulate water from the external water bath into boxes. The water bath was equipped with multiple air stones to ensure saturation, a 300 l h^{-1} Eheim pump to circulate water within the bath, and 3–5 300 W aquarium heaters (as needed depending on air temperature) to achieve acute heating. Up to two dogfish were tested at a time in separate boxes within the same water bath.

Upon placement in boxes, dogfish were habituated for at least 1 h before experimentation. Seawater flowed through the water bath during habituation to maintain ambient water temperatures similar to holding tank temperatures (∼11°C). After habituation, seawater flow to the water bath was shut off and heaters were turned on to begin acute thermal ramping with a target heating rate of 0.1°C min^{-1} (Bouyoucos et al., 2021). Water temperature of the bath was continuously monitored with a YSI Professional Plus meter (YSI Inc., Ohio, USA). The recorded starting temperature was 10.5±0.1°C for all trials, and the measured heating rate was 0.097±0.002°C min^{-1}. Dogfish were continuously monitored throughout trials, and ventilation rate (f_V; breaths min^{-1}) was measured every 10 min. An incremental temperature coefficient (Q_{10}, the sensitivity of a rate to temperature change) was calculated for f_V (f_{Vi}) every degree of temperature (T_i) increase as:

$$Q_{10} = \left(\frac{f_{V2}}{f_{V1}}\right)^{10/(T_2-T_1)}. \quad (1)$$

The agitation temperature was recorded as the temperature at which dogfish were observed to frequently change orientation in the box (i.e. toward or against inflowing water), which was interpreted as an avoidance behaviour. Definitions of behavioural endpoints for an agitation temperature are often specific to the experimental arena and study species. For consistency within the literature, our definition of the agitation temperature is similar to a study in cutthroat trout (*Oncorhynchus clarkia lewisi*) that were confined within respirometry chambers (Enders and Durhack, 2022). CT_{max} was recorded as the temperature at which dogfish exhibited muscle spasms, as indicated by rapid, lateral convulsions originating from the animal's trunk (Bouyoucos et al., 2020). The agitation temperature and CT_{max} were quantified by a single observer for the entire study. Practical limitations prevented video recording of trials to quantify the agitation temperature or CT_{max} using time-stamped video footage, as has been done in some (e.g. McDonnell and Chapman, 2015; Wells et al., 2016) but not all studies that quantify an agitation temperature (e.g. Enders and Durhack, 2022; Turko et al., 2020). As such, determination of agitation and CT_{max} was subjective, blinding was not possible and observer bias could not be accounted for experimentally. The agitation temperature occurs before CT_{max} (Enders and Durhack, 2022; McDonnell and Chapman, 2015), therefore, trials were terminated upon dogfish achieving CT_{max}. Upon termination of a trial, individual dogfish were tagged through the first dorsal fin with a numbered anchor tag for identification and were rapidly returned to their holding tank for recovery.

Cardiorespiratory thermal tolerance endpoints

The same dogfish used to measure whole-organism thermal tolerance endpoints were assayed for cardiorespiratory thermal tolerance endpoints. Dogfish were given at least 1 week to recover from CT_{max} trials to account for 'heat hardening' or improved thermal tolerance due to prior, recent exposure to acute warming. We were unable to determine if heat hardening occurred in dogfish; indeed, heat hardening has been shown to last for several days in some fishes (Bilyk et al., 2012; Maness and Hutchison, 1980), but can persist up to a week in other fishes (Grinder et al., 2020; Morgan et al., 2018). Cardiorespiratory thermal tolerance endpoints were determined by estimating heart rate (f_H; beats min^{-1}) from blood pressure traces measured in cannulated dogfish.

Dogfish were surgically cannulated following previously described methods (Acharya-Patel et al., 2018; Schoen et al., 2021). Briefly, dogfish were anesthetized in MS-222 (∼0.2 g l^{-1}) to the point where gross movements ceased yet ventilation continued (i.e. stage III). Following anaesthesia, dogfish were weighed and transferred to a V-board in supine position where a maintenance dose of MS-222 (∼0.1 g l^{-1}) was irrigated over the gills for the duration of the procedure. A pilot hole was made in the caudal peduncle, posterior to the anal fin, using a 16 gauge needle. A Touhy needle was then inserted into the puncture site and a length of PE-50 tubing (Intramedic, Fisher Scientific) was inserted into the caudal artery until the leading end was approximately 4–5 cm posterior of the pectoral girdle. The cannula was pre-filled with elasmobranch Ringer's solution (in mmol l^{-1}: 2 $CaCl_2{\cdot}2H_2O$, 5 glucose, 4 KCl, 3 $MgSO_4{\cdot}7H_2O$, 257 NaCl, 6 $NaHCO_3$, 0.1 NaH_2PO_4, 0.1 Na_2HPO_4, 7 Na_2SO_4, 80 trimethylamine oxide, 400 urea; pH 7.8 at 12°C; Deck et al., 2017) containing ammonium heparin (100 IU ml^{-1}), the trailing end was melted shut, and the cannula was secured to the caudal peduncle with silk sutures. Dogfish were then placed in the same boxes described in the 'Whole-organism thermal tolerance endpoints' section and allowed to recover for at least 24 h prior to experimentation (Acharya-Patel et al., 2018; Schoen et al., 2021).

f_H was estimated from blood pressure traces recorded using pressure transducers (ADInstruments SP 844, CO, USA) connected to a PowerLab data acquisition system (ADInstruments). Pressure transducers were calibrated before each use against a static column of water, with 0 cm H_2O set to the water's surface (Sandblom et al., 2009). Following recovery and habituation to boxes, cannulas were flushed with heparinised Ringer's solution and connected to a pressure transducer. Once stable blood pressure traces were observed for approximately 15 min, seawater flow to the water bath was turned off and heaters were turned on. The recorded starting temperature was 10.5±0.3°C for all trials, and the measured heating rate was 0.095±0.001°C min^{-1}. Because it was determined that the agitation temperature for dogfish was around 23°C, the water was only heated to approximately 23°C to ensure that dogfish did not harm themselves by ripping out their cannulas. Upon reaching 23°C, experiments were terminated by first detaching cannulas from pressure transducers. Then, cannulas were cut and sealed so that only ∼4–5 cm of tubing was exposed. Dogfish were then returned to their holding tank for recovery. Cannulas were intentionally left in dogfish so that cannulation of the venous or arterial vasculature could be later confirmed through dissection at the end of the experiment.

Blood pressure data were analysed using LabChart 5.1 software (ADInstruments) to estimate f_H (Acharya-Patel et al., 2018). T_{AB} was calculated using the 'broken stick method' (Yeager and Ultsch, 1989). Briefly, an Arrhenius plot (i.e. the natural logarithm of f_H as a function of the inverse of temperature in Kelvin multiplied by the Boltzmann constant) was fitted with a broken-line regression using the R package 'segmented' (https://CRAN.R-project.org/package=segmented), where the breakpoint was recorded as T_{AB}. T_{peak} was recorded as the temperature corresponding to the highest

Journal of Experimental Biology (2023) 226, jeb246304. doi:10.1242/jeb.246304

measured f_H. The arrhythmia temperature could not be reliably estimated from blood pressure traces as described previously (Heath and Hughes, 1973), so this metric was not measured. Finally, an incremental Q_{10} for f_H was calculated every 10 min, for every degree of temperature increase.

Objective 2: physiological responses at CT_{max}

Plasma biochemical responses to acute warming were measured for the same dogfish (n=7) undergoing CT_{max} experiments. Two blood samples (2 ml) were taken from each dogfish using ammonium heparin-washed 18 gauge needles; one immediately prior to habituation and another upon reaching CT_{max}. Whole blood was spun in duplicate in microcapillary tubes in a tabletop hematocrit centrifuge (2 min) to measure haematocrit (Hct). The remaining whole blood was spun for 2 min at 12,000 ***g*** to separate plasma from red blood cells. Plasma was decanted off and the remaining red blood cell pellet was frozen and thawed twice in liquid nitrogen for measurement of intracellular pH (pH_i; Schwieterman et al., 2021a, b) using an Orion ROSS Micro pH electrode (Thermo Fisher Scientific, MA, USA). The remaining plasma was used to measure potassium ion (K^+, mmol l^{-1}) and lactate concentrations (mmol l^{-1}). Plasma [K^+] was measured on a Thermo Fisher Scientific model iCE 3300 Atomic Absorption Spectrometer with samples diluted 1:250 in a 1% nitric acid solution containing 0.1 g l^{-1} caesium chloride as a matrix modifier. Plasma lactate concentration was measured spectrophotometrically (Morrison et al., 2020). Samples were deproteinated with two volumes of 6% perchloric acid and centrifuged (1 min at 12,000 ***g***). Ten microlitres of supernatant were combined with 200 µl of assay buffer (0.5 mmol l^{-1} NAD^+ in 200 mmol l^{-1} hydrazine sulphate, pH 9.5) to incubate for 5 min at room temperature. Then, 5 µl of lactate dehydrogenase (0.5 U $µl^{-1}$) or water (negative control) were added, and absorbance was measured initially and 60 min later at 340 nm in a microplate spectrophotometer (BioTek Powerwave, BioTek, VT, USA) with Gen5 software (Biotek). Lactate concentration was measured in duplicate for each sample and determined against a standard curve.

Objective 3: physiological responses at the agitation temperature

Tissue-specific transcript abundance and enzyme activity were measured in dogfish after experiencing acute warming to 23°C (n=5; mass=2.07±0.42 kg) or in 'sham' dogfish undergoing the same experimental procedure without experiencing acute warming (n=5; mass=1.99±0.31 kg). Seven of the dogfish used in this experiment had been used in previous experiments described in previous sections and were given at least 1 week to recover prior to experimentation; three naïve dogfish that had not undergone any previous experimentation were also used to increase sample size. All dogfish were tested using the identical experimental setup described for the previous objectives. For both groups, the recorded starting temperature was 12.7±0.4°C and the actual heating rate for the experimental group was 0.095±0.002°C min^{-1}. After either reaching 23°C or the equivalent time required to reach 23°C (i.e. the 'sham' group), dogfish were transferred from boxes and euthanized in an overdose of MS-222 (i.e.>0.25 g l^{-1}) in a water bath maintained at the respective final experimental temperature. Plasma was collected, and dogfish were then dissected for tissues that were stored in RNA later (Applied Biosystems, Thermo Fisher Scientific) at −20°C for subsequent molecular analysis or were flash-frozen in liquid nitrogen and stored at −80°C for subsequent enzyme activity analysis.

Transcript abundance

Total RNA was extracted from hypothalamus, gill filament, ventricle and white muscle using Trizol (Ambion, CA, USA), following the manufacturer's instructions. Integrity and purity of total RNA was determined via gel electrophoresis and NanoDrop One, respectively (Thermo Fisher Scientific, MS, USA). Total RNA was then treated with DNaseI per the manufacturer's instructions (Invitrogen, CA, USA). cDNA was synthesised from 1 µg total RNA (iScript cDNA synthesis kit; Bio-Rad, CA, USA) following the manufacturer's instructions.

Primers for genes of interest for real-time quantitative polymerase chain reaction (RT-qPCR) were deduced from whole genome shotgun sequences for *S. suckleyi* available from the National Center for Biotechnology Information (NCBI). Genes of interest were *hsp70* (accession number: JAOAMX010091476.1) and *hif1α* (JAOAMX010025045.1). Candidate reference genes were *rpl7* (JAOAMX010068065.1) and *actb*, which has been previously described for *S. suckleyi* (Nawata et al., 2015). Primers were designed in Primer-BLAST (https://www.ncbi.nlm.nih.gov/tools/primer-blast/) following manufacturer recommendations for SYBR Green master mix (Bio-Rad). Primer efficiency was determined for each gene within each tissue using serial dilutions of pooled cDNA. Primer sequences and efficiencies are provided in Table 1. RT-qPCR reactions were run with a Bio-Rad CRXConnect in 96-well plates. Reactions consisted of 2.5 µl of cDNA (5 ng $µl^{-1}$), 5.0 µl SYBR Green master mix, 1.25 or 2.5 µl of forward and reverse primer (200 or 400 nmol l^{-1} of each primer, respectively), and water up to a total volume of 10.0 µl. Cycling conditions were: 95°C for 10 min, and then 40 cycles of 95°C for 15 s and 60°C for 30 s, followed by a melt curve. Relative mRNA transcript abundances are presented as $2^{-\Delta Ct}$. Genes of interest (i.e. *hsp70*, *hif1α*) were normalized to the geometric mean of *actb* and *rpl7* (Hellemans et al., 2008; Vandesompele et al., 2002). For presentation, relative mRNA transcript abundance is presented relative to the mean of the 'sham' group (i.e. mean=1).

Enzyme activity

Ventricle, liver and white muscle tissues were assayed for citrate synthase (CS) and lactate dehydrogenase (LDH) activity. Assays were performed as outlined in Treberg et al. (2003). Tissues were weighed and homogenized in 10 volumes (1 mg:10 µl) of ice-cold homogenization buffer (50 mmol l^{-1} imidazole, pH 7.4) in a motorized bead mill homogenizer (VWR International, LLC.). Tissue homogenates were then centrifuged (10,000 ***g*** for 5 min at 4°C). The supernatant was then decanted off and diluted in water for use in kinetic assays, where 10 µl of sample was added to 200 µl of assay buffer. Samples were run in duplicate. Enzyme activity was determined spectrophotometrically at room temperature in clear, flat-bottom 96-well plates in a microplate spectrophotometer (BioTek Powerwave) with Gen5 software (Biotek).

Citrate synthase activity (i.e. the production of free CoA with 5,5′-dithio-bis-[2-nitrobenzoic acid]; DTNB) was monitored at 412 nm (extinction coefficient=6.22 $mmol^{-1}$ cm^{-1}) and LDH activity (i.e. the reduction of pyruvate with NADH) was monitored at 340 nm (extinction coefficient=13.6 $mmol^{-1}$ cm^{-1}). Assay conditions for CS (EC 2.3.3.1) were: 0.3 mmol l^{-1} acetyl-CoA, 0.1 mmol l^{-1} DTNB, 50 mmol l^{-1} imidazole (pH 8.0) and 0.5 mmol l^{-1} oxaloacetate (omitted for control). Assay conditions for LDH (1.1.1.27) were: 50 mmol l^{-1} imidazole (pH 7.4), 0.2 mmol l^{-1} NADH, and 1.0 mmol l^{-1} pyruvate (omitted for control). Enzyme activity was expressed in µmol min^{-1} g^{-1} wet weight. All chemicals were obtained from Sigma-Aldrich.

Table 1. Real-time quantitative polymerase chain reaction primer sequences, efficiencies and sources

Gene	Primer	Efficiency	Source
hsp70	F: AAGAAGAGGACGCTGGACGAAT R: GTTTCAGGTTACGAAGGGCCAG	102±2%	JAOAMX010091476.1
hif1α	F: AACGGGAACTTTCTGGATTCTGT R: GTTCTTCAGTCGCTTTGCCGT	99±8%	JAOAMX010025045.1
rpl7	F: CGCAAACTATACAGTGGGACCT R: AAATTGGGAAACCCCCAGGC	97±6%	JAOAMX010068065.1
actb	F: TGCACTGGACTTTGAACAGG R: TTCCACAGGATTCCATACCC	99±6%	Nawata et al., 2015

Forward (F) and reverse (R) primers are presented in 5′ to 3′ orientation. Efficiencies were determined for each gene in four different tissues and are listed as means±s.d.

Lactate concentration

At the end of the experiment, plasma was taken for analysis of lactate as described in objective 2. To quantify muscle lactate, white muscle samples were weighed and homogenized in 10 volumes (1 mg:10 µl) of ice-cold 6% perchloric acid in a motorized bead mill homogenizer (Milligan and Girard, 1993). The homogenate was centrifuged at 10,000 ***g*** for 5 min at 4°C. The supernatant was then used to quantify lactate concentration using the same assay described in objective 2. Muscle lactate was expressed in µmol g^{-1} wet weight.

Statistical analyses

All analyses were conducted using a Bayesian framework for interpretation. Models were fitted in R v. 1.7.4-1 (https://www.r-project.org/) using the package *brms* (https://CRAN.R-project.org/package=brms). For objective 1, Bayesian linear mixed effects models were fitted with temperature as a function of thermal tolerance trait (i.e. agitation temperature, CT_{max}, T_{AB}, T_{peak}) with dogfish ID as a random effect. Bayesian linear mixed effects models were also fitted with incremental Q_{10} for f_H or f_V as a function of temperature in 1°C bins as a nominal fixed effect with dogfish ID as a random effect. For objective 2, Bayesian linear mixed effects models were fitted with whole blood or plasma biochemical trait as a function of sampling timepoint (i.e. before vs after CT_{max}) with dogfish ID as a random effect. For objective 3, Bayesian linear models were fitted with fold-change transcript abundance or enzyme activity as a function of treatment (i.e. sham vs. warming). Bayesian linear models were also fitted with plasma or muscle lactate concentration as a function of treatment.

All models were fitted with Gaussian distribution and were run with four Hamiltonian Monte Carlo Markov Chains used over 4000 warm-up iterations and 20,000 total iterations (i.e. 64,000 total draws). Model validation was assessed through visual inspection of quantile–quantile plots of model residuals and plots of model residuals against fitted values. Model fit was assessed using the potential scale reduction statistic ($\hat{R}$), trace plots, and posterior predictive checks. Levels of fixed effects were compared using the *emmeans* R package (https://CRAN.R-project.org/package=emmeans), where levels were determined to be statistically significant if the 95% highest posterior density (HPD) interval of the mean difference between estimates did not contain zero.

RESULTS

Objective 1: thermal tolerance limits

Ventilation frequency increased throughout CT_{max} trials (Fig. 1A), with dogfish exhibiting an overall Q_{10} for f_V of 1.49±0.10. Incremental Q_{10} values for f_V remained stable throughout trials, except at 23 and 24°C, where incremental Q_{10} increased to nearly double the incremental Q_{10} at 11°C (Fig. 1B). Conversely, during heart rate measurement trials (Fig. 1C), incremental Q_{10} for f_H did not change throughout the entire trial (Fig. 1D), with an overall Q_{10} of 2.17±0.42. At the starting temperature of approximately 11°C, f_H was 26.5±4.5 beats min^{-1}, and the maximum f_H measured at T_{peak} was 53.9±9.9 beats min^{-1}. Population-level estimates for Bayesian linear mixed effects models are presented in Table S1.

CT_{max} was measured in seven dogfish and was 24.6±0.3°C (mean±s.e.m.). All dogfish exhibited a clear avoidance response during acute warming and demonstrated an agitation temperature of 23.2±0.4°C. Upon dissection, it was determined that only six of seven dogfish were properly cannulated in the caudal artery; therefore, heart rate data from the dogfish with a venous cannula was excluded from further analyses. Of the six dogfish with arterial cannulas, a clear T_{peak} at 22.6±0.3°C was recorded. Interestingly, only four of six dogfish exhibited signs of bradycardia and, therefore, a T_{AB}. Recorded T_{AB} was 21.5±0.5°C.

Dogfish exhibited a progression of thermal tolerance limits (Fig. 2). The agitation temperature was equal to T_{peak} and higher than T_{AB}. However, T_{AB} and T_{peak} were not found to be significantly different. CT_{max} was significantly higher than all other thermal limits. Therefore, T_{AB} seemed to precede the agitation temperature, which occurred at T_{peak}, while all metrics preceded CT_{max}. Population-level estimates for Bayesian linear mixed effects models are presented in Table S2.

Objective 2: physiological responses at CT_{max}

In response to acute warming to CT_{max}, Hct was unaffected (Fig. 3A). Overall, Hct was 0.15±0.05 (mean±s.d.). Intracellular pH decreased from 7.06±0.11 to 6.90±0.14 in response to acute warming to CT_{max} (Fig. 3B). As with Hct, $[K^+]$ was unaffected, and averaged 7.12±2.97 mmol l^{-1} (Fig. 3C). Plasma lactate concentration increased considerably from 0.32±0.18 mmol l^{-1} to 10.59±1.60 mmol l^{-1} (Fig. 3D). Population-level estimates for Bayesian linear mixed effects models are presented in Table S3.

Objective 3: physiological responses at the agitation temperature

Dogfish exhibited tissue- and transcript-specific responses to acute warming to the agitation temperature. Relative transcript abundance of *hsp70* was notably higher in hypothalamus (Fig. 4A), gill filament (Fig. 4C) and ventricle (Fig. 4E) of dogfish subjected to acute warming relative to sham treated dogfish. Conversely, *hsp70* relative abundance was not different between treatment groups in white muscle (Fig. 4G). There were no apparent differences in *hif1α* between dogfish in both treatment groups in any tissue (Fig. 4B,D,F,H). Population-level estimates for Bayesian linear models are presented in Table S4.

Journal of Experimental Biology (2023) 226, jeb246304. doi:10.1242/jeb.246304

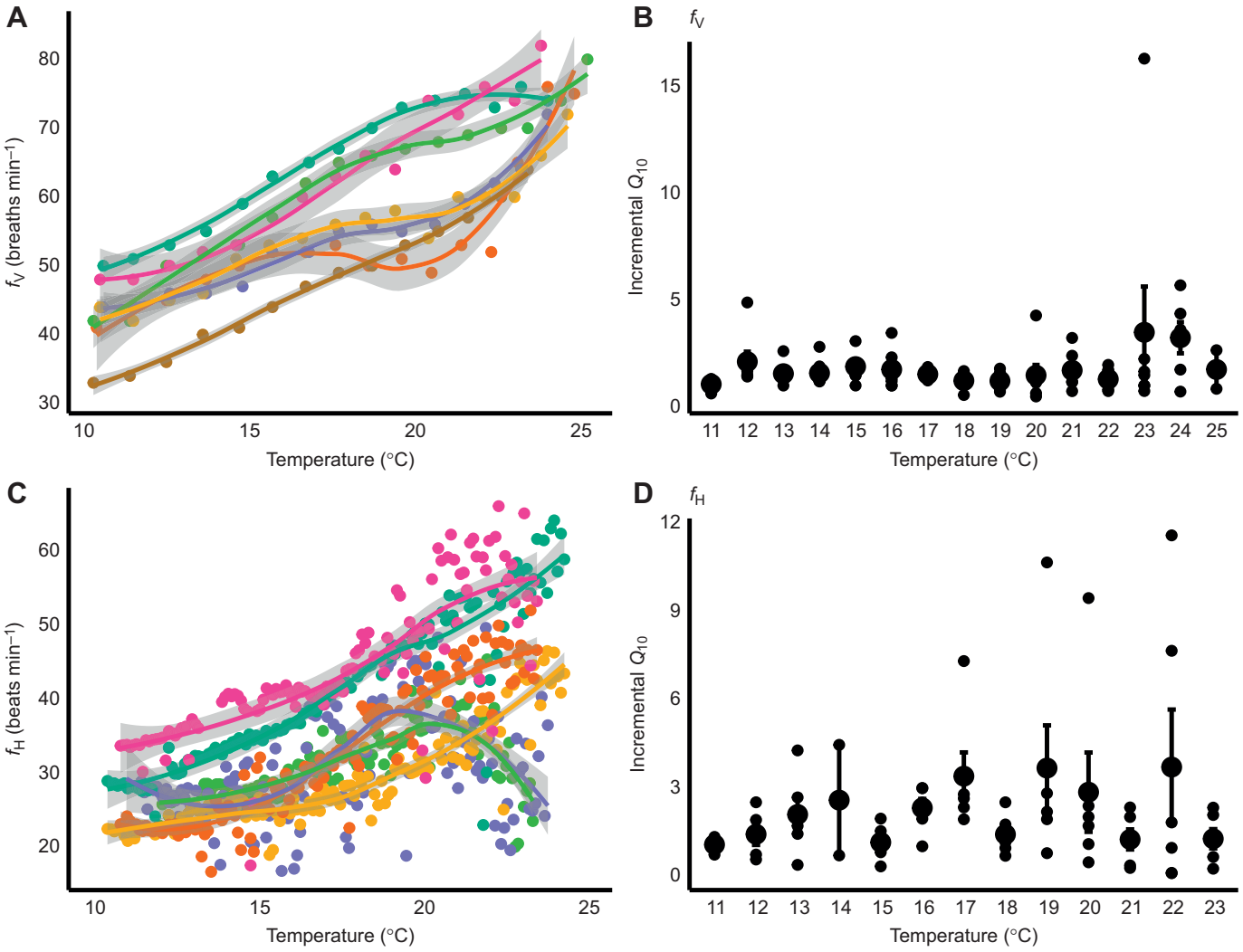

Fig. 1. Effects of temperature increase on cardiorespiratory performance in Pacific spiny dogfish (*Squalus suckleyi*). Dogfish were exposed to an acute temperature increase and monitored for ventilation frequency (f_V; A,B) and heart rate (f_H; C,D). Incremental temperature coefficients (Q_{10}) were calculated for each degree of temperature increase. In the left panels, lines are fitted to f_V or f_H for individual sharks (n=7 and 6, respectively), where points represent individual observations, shading represents 95% confidence intervals and colours represent different individual sharks. In the right panels, raw data are depicted as means±s.e.m., where points are incremental Q_{10} values from individual dogfish.

CS (Fig. 5A) and LDH (Fig. 5B) activity in the ventricle did not differ between sham handled and acutely warmed dogfish. Similarly, CS (Fig. 5C) and LDH (Fig. 5D) activity in the liver did not differ between sham handled and acutely warmed dogfish. In white muscle, however, CS activity was significantly higher in acutely warmed dogfish (Fig. 5E). Acutely warmed dogfish had a white muscle CS activity of 0.46±0.18 µmol min^{-1} g^{-1}, whereas sham dogfish white muscle CS activity was 0.25±0.05 µmol min^{-1} g^{-1}. Conversely, white muscle LDH activity did not differ between sham and acutely warmed dogfish (Fig. 5F). Population-level estimates for Bayesian linear models are presented in Table S5.

Plasma lactate did not differ between sham handled and acutely warmed dogfish (Fig. 6A); however, concentrations in sham (3.49±0.85 mmol l^{-1}) and warmed (3.09±0.58 mmol l^{-1}) dogfish were relatively higher than values recorded before CT_{max} (0.32±0.18 mmol l^{-1}; Fig. 3D). White muscle lactate did not differ between sham handled (12.57±5.24 µmol g^{-1}) and acutely warmed (10.38±1.71 µmol g^{-1}) dogfish (Fig. 6B). Population-level estimates for Bayesian linear models are presented in Table S6.

DISCUSSION

The present study represents the first examination of underlying molecular, biochemical and cardiorespiratory responses occurring at the agitation temperature in any fish. Our results indicate that, in spiny dogfish, the agitation temperature is characterised by maximal cardiorespiratory performance (i.e. peak heart rate and high thermal sensitivity of respiratory rate), tissue-specific signs of thermal – but not hypoxemic – cellular stress, and tissue-specific increases in aerobic enzyme activity. There were no signs of a secondary stress response at the agitation temperature; however, there were pronounced signs of secondary stress resembling metabolic acidosis, but not hyperkalemia or decreased oxygen transport, at CT_{max}. These results suggest that oxygen supply capacity is maintained at the agitation temperature and that initiation of the cellular stress response may be a proximal driver of observed avoidance behaviours (i.e. agitation). Together, these data provide partial support for our hypothesis, in that a cellular stress response occurred at the agitation temperature, and that cardiorespiratory performance was maximised rather than declining. As such, these data may reflect Jensen's inequality, where the behaviourally

Journal of Experimental Biology (2023) 226, jeb246304. doi:10.1242/jeb.246304

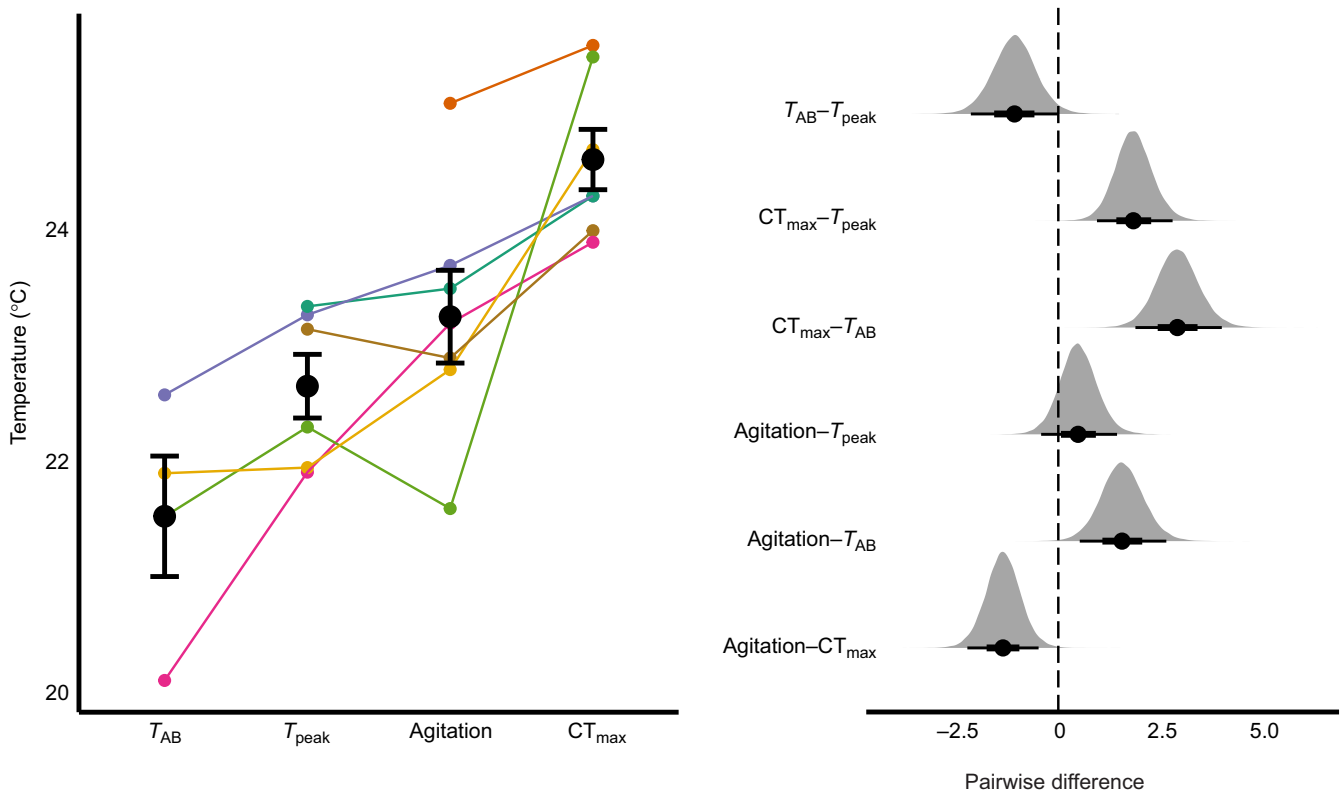

Fig. 2. Thermal tolerance traits of Pacific spiny dogfish (*S. suckleyi*). Dogfish were exposed to an acute temperature increase to quantify critical thermal maxima (CT_{max}; n=7), the agitation temperature (n=7), temperature of peak heartrate (T_{peak}; n=6) and the Arrhenius breakpoint temperature (T_{AB}; n=4). Graph on the left shows the raw data (means±s.e.m.), where points represent thermal tolerance trait values from individual dogfish. Colours represent different individual sharks and lines connect points within individuals. Thermal tolerance traits were compared with Bayesian linear mixed effects models. Highest posterior density (HPD) distributions for comparisons between each thermal tolerance trait are shown on the right. HPD distributions are described by the mean (dot), 66% HPD interval (thick line) and 95% HPD interval (thin line). Comparisons whose 95% HPD intervals do not overlap zero (vertical dashed line) are statistically significant.

preferred temperature is often lower than the optimal temperature where performance of a biological trait is maximised, owing to a precipitous decline in performance experienced with further warming (Martin and Huey, 2008).

Dogfish demonstrated a clear agitation temperature occurring prior to CT_{max}. Although the distinction between *S. suckleyi* and its congener, *S. acanthias*, is unclear in the literature prior to 2010 (Ebert et al., 2010), upper thermal limits have not been characterized in either species. One study held *S. suckleyi* at 12–22°C for 6 h to measure oxygen uptake rates and reported no mortality (Giacomin et al., 2017). This study suggested that CT_{max} in *S. suckleyi* may exceed 22°C because most dogfish could not maintain an upright orientation for a full 6 h at 22°C (Giacomin et al., 2017), and attempts to keep dogfish at higher temperatures were unsuccessful (C. M. Wood, personal communication). The present study represents the first report of an agitation temperature in an elasmobranch fish; although, others have reported the highest temperature experienced in a temperature preference experiment in epaulette sharks as the upper threshold temperature (Nay et al., 2021). The difference between CT_{max} and the agitation temperature (the 'CT_{max}-agitation window') has been proposed as another thermal tolerance metric akin to thermal safety margins (i.e. CT_{max} minus acclimation temperature), where a smaller CT_{max}-agitation window implies greater thermal tolerance (Wells et al., 2016). Dogfish exhibited a relatively narrow CT_{max}-agitation window of approximately 1.4°C in comparison to a large thermal safety margin of nearly 15°C. Thus, such a small CT_{max}-agitation window may suggest that dogfish are relatively temperature-tolerant; alternatively, dogfish experiencing acute temperature change may risk experiencing warming to within degrees of their CT_{max}.

Dogfish exhibited signs of peak cardiorespiratory performance during acute warming over a thermal window of 10–23°C. All dogfish exhibited tachycardia with a clear T_{peak} and most, but not all, dogfish experienced bradycardia with a clear T_{AB}. Prior to acute warming at ∼11°C, f_H in dogfish was similar, albeit higher than f_H in cannulated *S. suckleyi* measured at 10°C (26.5 vs. 19.0 beats min^{-1}; Sandblom et al., 2009). Acute warming produced moderate increases in f_V (Q_{10}=1.49) and f_H (Q_{10}=2.17) up to a peak f_H of 53.4 beats min^{-1}. In comparison, previous research on *S. suckleyi* demonstrated a Q_{10} for f_H at 10–16°C of 2.2 and a Q_{10} for oxygen uptake rate at 7.5–22.0°C of 1.76 (Giacomin et al., 2017; Sandblom et al., 2009). Incremental Q_{10} for f_V was unchanged until 23–24°C, which occurs between the agitation temperature and CT_{max}, possibly indicative of increased oxygen demands. Indeed, dogfish exhibited higher CS activity in white muscle at the agitation temperature relative to sharks that did not undergo warming, and plasma lactate nearly tripled from the agitation temperature to CT_{max}, indicating an increase in the use of anaerobic metabolic pathways. In contrast to f_V, incremental Q_{10} for f_H did not change in response to acute warming. f_H may have followed a similar trend as f_V if cannulated sharks had been exposed to temperatures above 23°C. Alternatively, trends in f_H and f_H metrics (i.e. T_{peak} and T_{AB})

Journal of Experimental Biology (2023) 226, jeb246304. doi:10.1242/jeb.246304

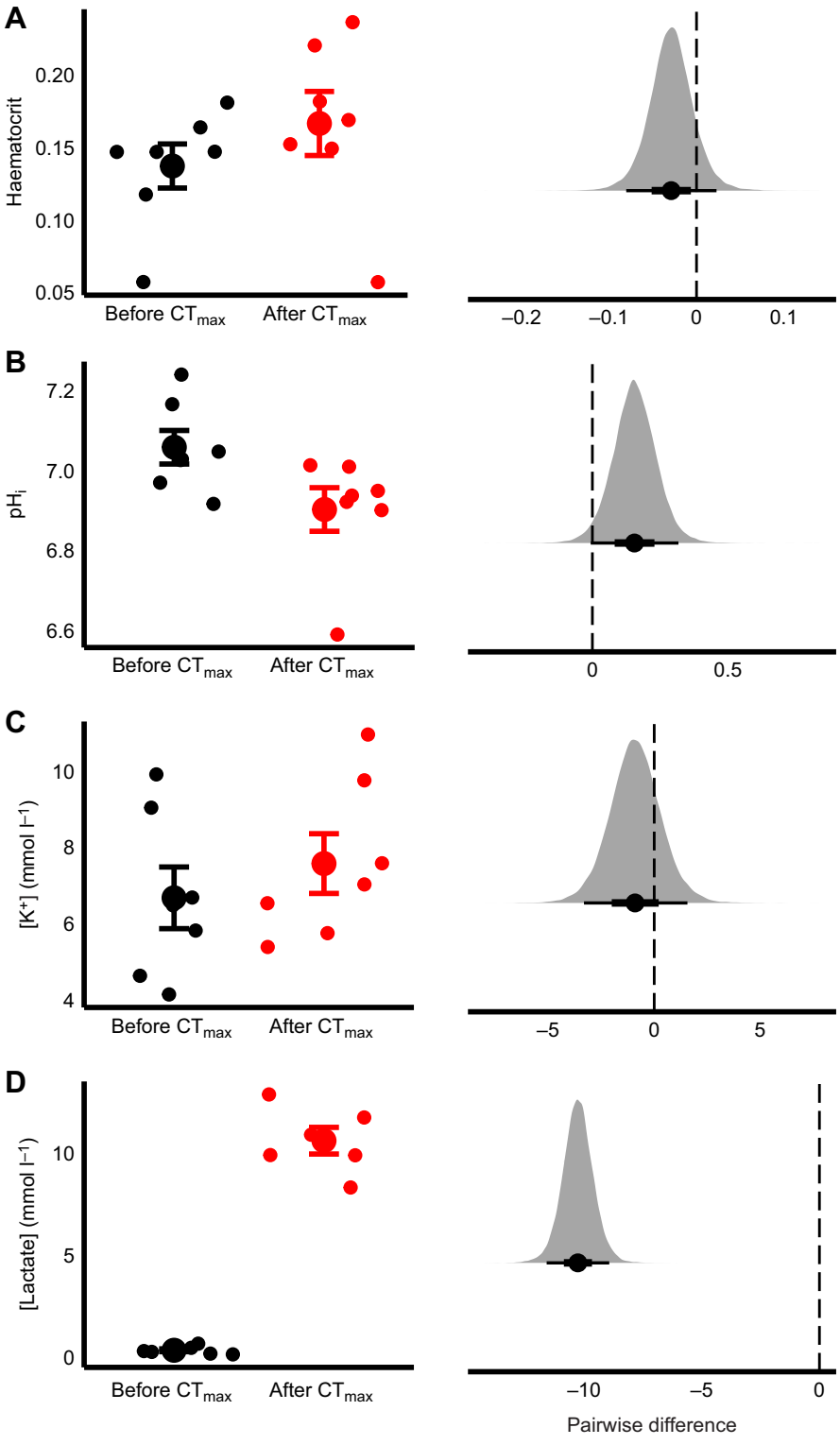

Fig. 3. Whole blood and plasma biochemical responses to acute temperature increase in Pacific spiny dogfish (*S. suckleyi*). Blood was sampled from individual dogfish (n=7) before (black) and after (red) exposure to an acute temperature increase to quantify critical thermal maxima (CT_{max}). Lefthand panels depict raw data (means±s.e.m.), where points represent thermal tolerance trait values from individual dogfish. Values for haematocrit (A), intracellular pH (pH_i; B), plasma potassium (K^+) concentration (C) and plasma lactate concentration (D) were compared with Bayesian linear mixed effects models. Right panels depict HPD distributions for comparisons between values sampled before or after dogfish reached CT_{max}. HPD distributions are described by the mean (dot), 66% HPD interval (thick line) and 95% HPD interval (thin line). Comparisons whose 95% HPD intervals do not overlap zero (vertical dashed line) are statistically significant.

may reflect the experimental design, where temperature dependence of f_H and not maximum f_H ($f_{H,max}$) was measured. In teleost and elasmobranch fishes, $f_{H,max}$ is often measured by stimulating hearts with atropine as a means to standardise f_H across individuals (Acharya-Patel et al., 2018; Casselman et al., 2012); indeed, such intraspecific variation in temperature-dependent f_H was apparent in dogfish. In fishes stimulated with atropine, an incremental Q_{10} for $f_{H,max}$ typically decreases with increasing temperature until arrhythmias occur (Gilbert et al., 2020), whereas incremental Q_{10} for f_H did not change with warming in dogfish. Bradycardia and arrhythmia typically occur within degrees of CT_{max} (Chen et al., 2013; Ekström et al., 2014; Gilbert et al., 2020); however, it is unclear whether dogfish would have exhibited arrhythmia between 23 and 25°C, immediately prior to exhibiting CT_{max}.

Acute warming to the agitation temperature was characterized by increased aerobic metabolic activity. In dogfish, the agitation

Journal of Experimental Biology (2023) 226, jeb246304. doi:10.1242/jeb.246304

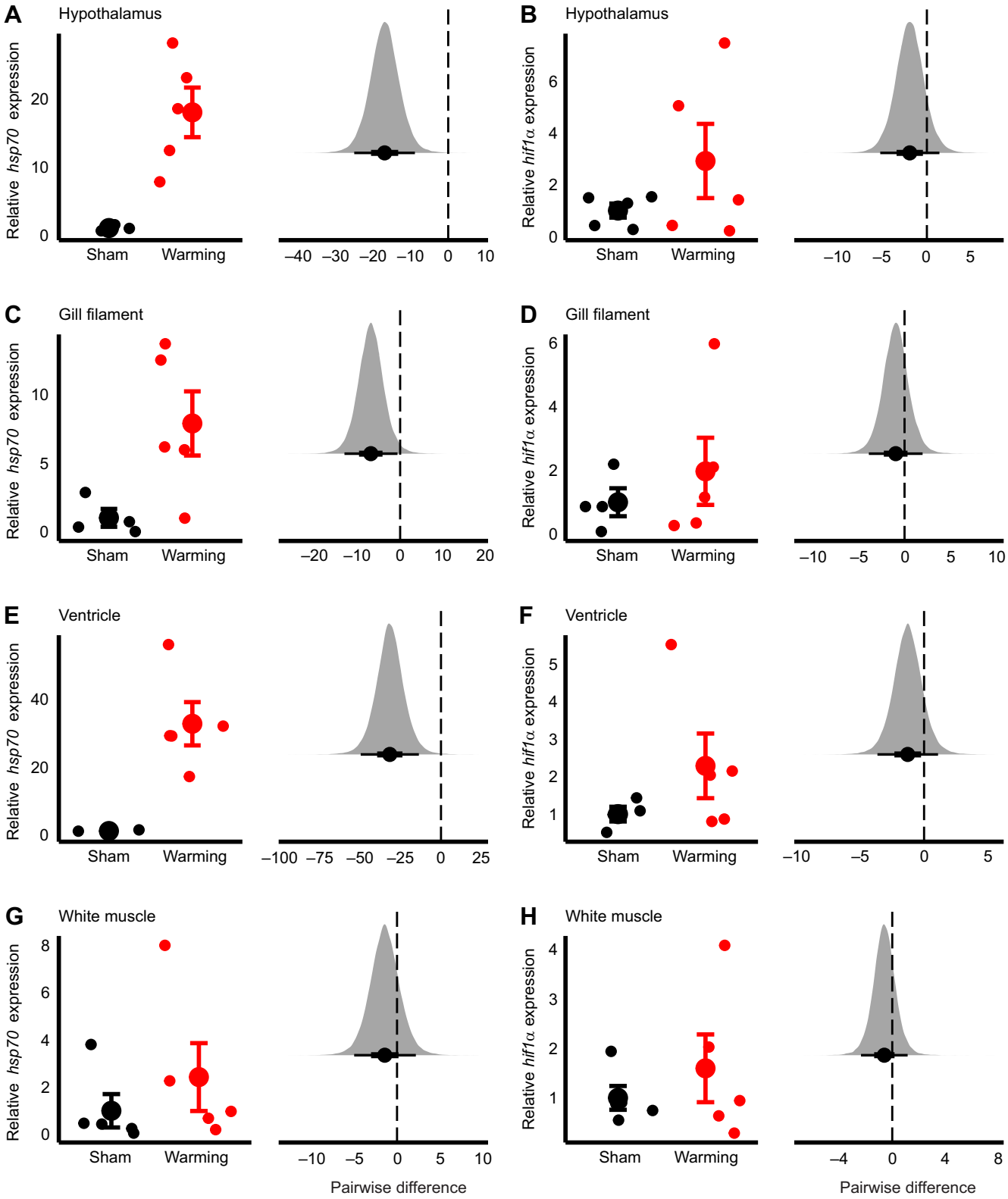

Fig. 4. Effects of acute temperature increase on relative mRNA transcript abundance in Pacific spiny dogfish (*S. suckleyi*). Hypothalamus (A,B), gill filament (C,D), ventricle (E,F) and white muscle (G,H) were sampled from individual dogfish exposed to an acute temperature increase ('warming'; red; n=5) or handled without warming ('sham'; black; n=5). Within panels, plots on the left depict raw data (means±s.e.m.), where points represent relative mRNA transcript abundance from individual dogfish. Genes of interest *hsp70* (A,C,E,G) and *hif1α* (B,D,F,H) are presented as $2^{-\Delta Ct}$ and normalized to the geometric mean of *actb* and *rpl7* using the geNorm method. Values were compared with Bayesian linear models. HPD distributions for comparisons between sham or warming dogfish are shown to the right. HPD distributions are described by the mean (dot), 66% HPD interval (thick line) and 95% HPD interval (thin line). Comparisons whose 95% HPD intervals do not overlap zero (vertical dashed line) are statistically significant.

Journal of Experimental Biology (2023) 226, jeb246304. doi:10.1242/jeb.246304

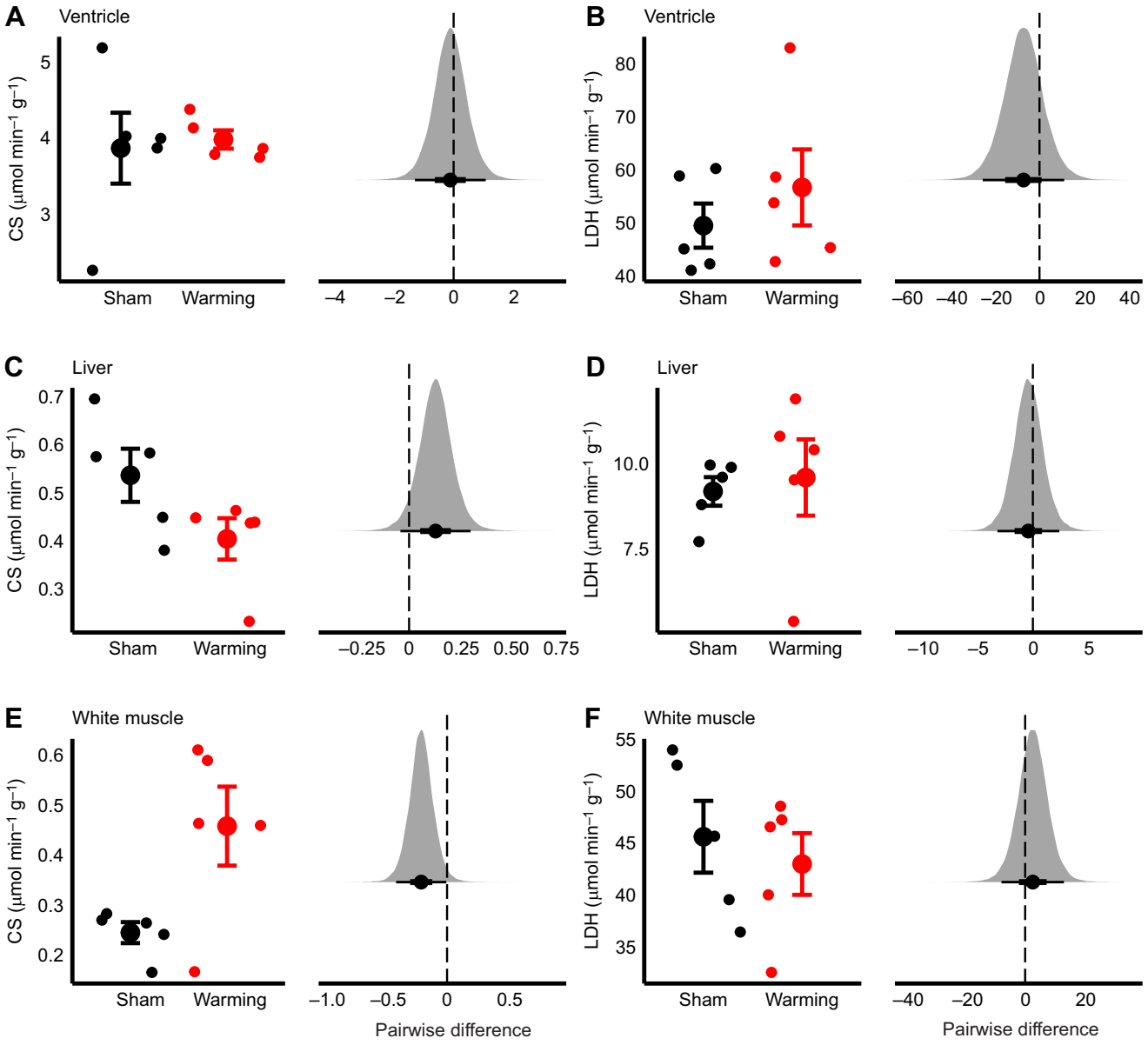

Fig. 5. Effects of acute temperature increase on enzyme activity in Pacific spiny dogfish (*S. suckleyi*). Ventricle (A,B), liver (C,D), white muscle (E,F) were sampled from individual dogfish exposed to an acute temperature increase ('warming'; red; *n*=5) or handled without warming ('sham'; black; *n*=5). Within panels, plots on the left depict raw data (means±s.e.m.), where points represent citrate synthase (CS; A,C,E) or lactate dehydrogenase (LDH; B,D,F) activities from individual dogfish. Values were compared with Bayesian linear models. HPD distributions for comparisons between sham or warming dogfish are shown on the right. HPD distributions are described by the mean (dot), 66% HPD interval (thick line) and 95% HPD interval (thin line). Comparisons whose 95% HPD intervals do not overlap zero (vertical dashed line) are statistically significant.

temperature was statistically similar to T_{peak}. In addition, CS activity was maintained in critical tissues and elevated in peripheral white muscle, which suggests that dogfish were able to rapidly increase CS abundance in white muscle over the course of several hours. Comparatively, previous work has demonstrated tissue-specific increases or no change in CS activity in response to acute warming to CT_{max} in various teleosts (e.g. Illing et al., 2020; O'Brien et al., 2018). Together, these data suggest that dogfish may have been performing at their maximal aerobic potential. In further support of this notion, LDH activity did not change in heart, liver, and white muscle, and lactate did not accumulate in the plasma or white muscle, suggesting that dogfish were able to meet their energy demand during acute warming within their aerobic scope. It is noteworthy that plasma lactate concentrations in dogfish acutely warmed to the agitation temperature were higher than values for minimally stressed dogfish and lower than values for dogfish at CT_{max}. However, there was no difference in plasma or muscle lactate concentrations between dogfish warmed to the agitation temperature and those exposed to a sham procedure; thus, the moderately elevated lactate is possibly an artefact of handling stress. Indeed, lactate concentrations often increase in fishes in response to thermal stress, often measured at or after CT_{max} (e.g. Murchie et al., 2011; O'Brien et al., 2018; Zhang and Kieffer, 2014). Thus, an oxygen limitation of the agitation temperature in dogfish is not apparent from these data; although, effects of hypoxia on the agitation temperature have been documented in other fishes (McDonnell et al., 2019, 2021; Potts et al., 2021). Therefore, these data suggest that dogfish do not increase their reliance on

Journal of Experimental Biology (2023) 226, jeb246304. doi:10.1242/jeb.246304

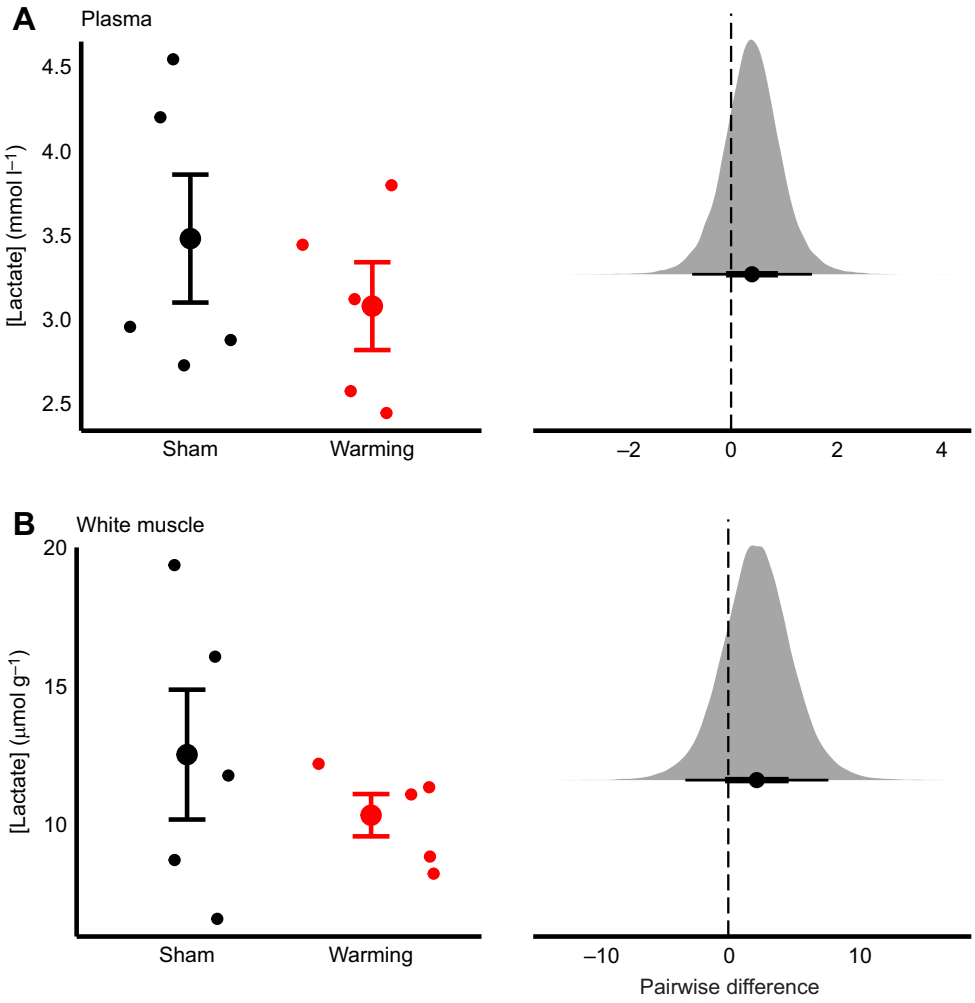

Fig. 6. Effects of acute temperature increase on plasma and muscle lactate concentrations in Pacific spiny dogfish (*S. suckleyi*). Plasma (A) and white muscle (B) were sampled from individual dogfish exposed to an acute temperature increase ('warming'; red; *n*=5) or handled without warming ('sham'; black; *n*=5). Within panels, plots on the left depict raw data (means±s.e.m.), where points represent lactate concentrations from individual dogfish. Values were compared with Bayesian linear models. HPD distributions for comparisons between sham or warming dogfish are shown on the right. HPD distributions are described by the mean (dot), 66% HPD interval (thick line) and 95% HPD interval (thin line). Comparisons whose 95% HPD intervals do not overlap zero (vertical dashed line) are statistically significant.

anaerobic metabolic pathways at the agitation temperature when at rest, but may do so with further warming to CT_{max} or when swimming (Nati et al., 2023; Sandrelli and Gamperl, 2023).

Dogfish exhibited signs of thermal cellular stress at the agitation temperature. Relative *hsp70* transcript abundance was higher in brain, gill and heart tissue at the agitation temperature relative to levels in sham-handled dogfish, whereas no difference was noted in *hif1α* relative abundance in these tissues, or for either transcript in white muscle. Heat shock protein responses to acute warming have been demonstrated in *S. acanthias* (Bockus et al., 2020; Kolhatkar et al., 2014). These studies further tested whether TMAO production increased with thermal stress, wherein TMAO is hypothesised to function similarly to Hsp70 as a protein chaperone. However, because it has been demonstrated that TMAO inactivates the *hsp70* response, it is unlikely that *S. suckleyi* in the present study were producing appreciable amounts of TMAO over the relatively short duration of acute heating (Kolhatkar et al., 2014; Villalobos and Renfro, 2007). Furthermore, as TMAO is largely derived from diet (Treberg and Driedzic, 2006), it is reasonable to hypothesize that TMAO acts as a chaperone during chronic heat stress, whereas Hsp70 is a chaperone under acute heat stress. Notably, *hsp70* transcript abundance increased in organs whose upper thermal limits are thought to contribute to whole-organism thermal limits: the brain and heart (Andreassen et al., 2022; Anttila et al., 2023). Indeed, a heat shock protein response in these tissues and possibly others (e.g. gills) may coincide with the initiation of avoidance behaviours at higher temperatures, particularly if failure of these organs may contribute to heat failure or 'ecological death' of the organism. In addition, the absence of a Hif1α response suggests that various tissues did not experience stress from heat-induced hypoxemia. However, it is not clear whether a Hif1α response could occur with warming above the agitation temperature. In various fishes, *hif1α* transcript abundance has been shown to increase at CT_{max} (Earhart et al., 2023; O'Brien et al., 2020); although, links between Hif1α and CT_{max} are equivocal (Joyce and Perry, 2020). Cellular stress may be connected to the neuroendocrine stress response; however, *S. suckleyi* has been shown not to exhibit a catecholaminergic response to acute warming but only up to 16°C (Sandblom et al., 2009).

At CT_{max}, dogfish exhibited signs of a secondary stress response. Dogfish exhibited maximal f_V and metabolic acidosis, characterised by reduced intracellular pH and increased plasma lactate. While these data do not test oxygen-limitation of CT_{max}, per se, accumulated plasma lactate values in dogfish at CT_{max} very closely match plasma lactate values in *S. suckleyi* exposed to moderate hypoxia (20% air O_2 saturation or ∼37 torr) for 2 h (Zimmer and Wood, 2014), which was the approximate duration of CT_{max} trials for dogfish. Haematocrit was unaffected by acute warming but there is little mechanistic support for increases in Hct in elasmobranch fishes (Opdyke and Opdyke, 1971; Schwieterman et al., 2021a). Plasma $[K^+]$ was also unaffected by rapid warming to CT_{max}. Together, temperature, acidosis, and hyperkalemia (i.e.

$[K^+]$>10 mmol l^{-1}) are thought to act synergistically to exert negative effects on cardiac performance (Schwieterman et al., 2021b). From our experimental design, it is unclear whether temperatures above the agitation temperature negatively impacted cardiorespiratory performance; indeed, f_H was maximised, suggesting that dogfish could either maintain f_H at its peak or exhibit bradycardia and/or arrhythmia. Plasma $[K^+]$ was within the range of concentrations reported to have no effect on isolated cardiomyocyte function in other elasmobranch fishes (Schwieterman et al., 2021b). In *S. suckleyi*, f_H in excised hearts (i.e. *ex vivo*) was reduced in hypercapnia (15% CO_2, pH ∼6.0) but restored when buffered with sodium bicarbonate to a pH of ∼7.1 (Lo et al., 2021), which aligns with pH_i measured in dogfish at CT_{max} (pH_i=6.9). Therefore, further research is warranted to determine cardiovascular performance at temperatures approaching CT_{max} in elasmobranchs, and the biochemical conditions that may contribute to cardiac collapse.

In conclusion, the present study demonstrates numerous, unique physiological responses occurring at whole-organism upper thermal limits in an elasmobranch fish. By testing physiological responses at multiple levels of biological organisation, this study provides partial mechanistic support for the hypothesis that the agitation temperature is associated with the cellular stress response and is not an oxygen-limited thermal tolerance trait. The present study also supports the notion that the brain and heart are important organs responsible for setting whole-organism thermal limits, and that further investigation of thermal tolerance of these organs, particularly the brain, can elucidate further mechanistic underpinnings of whole-organism thermal tolerance. Further research is warranted in elasmobranchs to begin to describe mechanisms of thermal tolerance in these fishes. Indeed, the unique thermal physiology of elasmobranchs is thought to constrain their biogeographic ranges relative to teleosts (Watanabe and Payne, 2023) and climate change is increasingly being recognized as a threat to elasmobranchs worldwide (Dulvy et al., 2014, 2021). Therefore, further mechanistic research would be a meaningful contribution to comparative thermal physiology while also informing species management through the lens of conservation physiology.

Acknowledgements
The authors thank Jenna Drummond and Ameera Kingra for assistance in the field and laboratory, and Dr Matt Thorstensen for guidance in Bayesian statistics. Tao Eastham and animal care staff at the Bamfield Marine Sciences Centre provided logistical support. The Bamfield Marine Sciences Centre sits within the traditional territory of the Huu-ay-aht First Nations and the University of Manitoba campuses are located on the original lands of the Anishinaabeg, Cree, Oji-Cree, Dakota, and Dene peoples, and on the homeland of the Métis Nation.

Competing interests
The authors declare no competing or financial interests.

Author contributions
Conceptualization: I.A.B., A.M.W., K.M.J., W.G.A.; Methodology: I.A.B., A.M.W., W.G.A.; Formal analysis: I.A.B.; Investigation: I.A.B., A.M.W.; Resources: W.G.A.; Writing - original draft: I.A.B.; Writing - review & editing: I.A.B., A.M.W., K.M.J., W.G.A.; Supervision: W.G.A.; Funding acquisition: W.G.A.

Funding
The authors were supported by a Natural Sciences and Engineering Research Council of Canada (NSERC)/Manitoba Hydro Industrial Research Chair grant (479350/1) and an NSERC Discovery grant (05328) awarded to W.G.A. A.M.W. was supported by an NSERC PDF award. Fieldwork was also supported by the University of Manitoba Faculty of Science Fieldwork Support program.

Data availability
Raw data are available on Mendeley at: https://data.mendeley.com/datasets/xk9bzb6kbc/1.

ECR Spotlight
This article has an associated ECR Spotlight interview with Ian Bouyoucos.

References
Acharya-Patel, N., Deck, C. A. and Milsom, W. K. (2018). Cardiorespiratory interactions in the Pacific spiny dogfish, *Squalus suckleyi*. *J. Exp. Biol.* **221**, jeb183830. doi:10.1242/jeb.183830

Andreassen, A. H., Hall, P., Khatibzadeh, P., Jutfelt, F. and Kermen, F. (2022). Brain dysfunction during warming is linked to oxygen limitation in larval zebrafish. *Proc. Natl. Acad. Sci. USA* **119**, e2207052119. doi:10.1073/pnas.2207052119

Anttila, K., Dhillon, R. S., Boulding, E. G., Farrell, A. P., Glebe, B. D., Elliott, J. A. K., Wolters, W. R. and Schulte, P. M. (2013). Variation in temperature tolerance among families of Atlantic salmon (*Salmo salar*) is associated with hypoxia tolerance, ventricle size and myoglobin level. *J. Exp. Biol.* **216**, 1183-1190. doi:10.1242/jeb.080556

Anttila, K., Mauduit, F., Kanerva, M., Götting, M., Nikinmaa, M. and Claireaux, G. (2023). Cardiovascular oxygen transport and peripheral oxygen extraction capacity contribute to acute heat tolerance in European seabass. *Comp. Biochem. Physiol. A Mol. Integr. Physiol.* **275**, 111340. doi:10.1016/j.cbpa.2022.111340

Becker, C. D. and Genoway, R. G. (1979). Evaluation of the critical thermal maximum for determining thermal tolerance of freshwater fish. *Environ. Biol. Fishes* **4**, 245-256. doi:10.1007/BF00005481

Beitinger, T., Bennett, W. and McCauley, R. (2000). Temperature tolerances of North American freshwater fishes exposed to dynamic changes in temperature. *Environ. Biol. Fishes* **58**, 237-275. doi:10.1023/A:1007676325825

Bilyk, K. T., Evans, C. W. and DeVries, A. L. (2012). Heat hardening in Antarctic notothenioid fishes. *Polar Biol.* **35**, 1447-1451. doi:10.1007/s00300-012-1189-0

Blasco, F. R., Esbaugh, A. J., Killen, S. S., Rantin, F. T., Taylor, E. W. and McKenzie, D. J. (2020). Using aerobic exercise to evaluate sub-lethal tolerance of acute warming in fishes. *J. Exp. Biol.* **223**, jeb218602. doi:10.1242/jeb.218602

Bockus, A. B., LaBreck, C. J., Camberg, J. L., Collie, J. S. and Seibel, B. A. (2020). Thermal range and physiological tolerance mechanisms in two shark species from the northwest atlantic. *Biol. Bull.* **238**, 131-144. doi:10.1086/708718

Bouyoucos, I. A., Morrison, P. R., Weideli, O. C., Jacquesson, E., Planes, S., Simpfendorfer, C. A., Brauner, C. J. and Rummer, J. L. (2020). Thermal tolerance and hypoxia tolerance are associated in blacktip reef shark (*Carcharhinus melanopterus*) neonates. *J. Exp. Biol.* **223**, jeb221937. doi:10.1242/jeb.221937

Bouyoucos, I. A., Trujillo, J. E., Weideli, O. C., Nakamura, N., Mourier, J., Planes, S., Simpfendorfer, C. A. and Rummer, J. L. (2021). Investigating links between thermal tolerance and oxygen supply capacity in shark neonates from a hyperoxic tropical environment. *Sci. Total Environ.* **782**, 146854. doi:10.1016/j.scitotenv.2021.146854

Casselman, M. T., Anttila, K. and Farrell, A. P. (2012). Using maximum heart rate as a rapid screening tool to determine optimum temperature for aerobic scope in Pacific salmon Oncorhynchus spp. *J. Fish Biol.* **80**, 358-377. doi:10.1111/j.1095-8649.2011.03182.x

Chen, Z., Anttila, K., Wu, J., Whitney, C. K., Hinch, S. G. and Farrell, A. P. (2013). Optimum and maximum temperatures of sockeye salmon (*Oncorhynchus nerka*) populations hatched at different temperatures. *Can. J. Zool.* **91**, 265-274. doi:10.1139/cjz-2012-0300

Chung, D. J. and Schulte, P. M. (2020). Mitochondria and the thermal limits of ectotherms. *J. Exp. Biol.* **223**, jeb227801. doi:10.1242/jeb.227801

Dabruzzi, T. F., Bennett, W. A., Rummer, J. L. and Fangue, N. A. (2013). Juvenile ribbontail stingray, *Taeniura lymma* (Forsskål, 1775) (Chondrichthyes, Dasyatidae), demonstrate a unique suite of physiological adaptations to survive hyperthermic nursery conditions. *Hydrobiologia* **701**, 37-49. doi:10.1007/s10750-012-1249-z

Deck, C. A., Anderson, W. G., Conlon, J. M. and Walsh, P. J. (2017). The activity of the rectal gland of the North Pacific spiny dogfish *Squalus suckleyi* is glucose dependent and stimulated by glucagon-like peptide-1. *J. Comp. Physiol. B Biochem. Syst. Environ. Physiol* **187**, 1155-1161. doi:10.1007/s00360-017-1102-9

Desforges, J. E., Birnie-Gauvin, K., Jutfelt, F., Gilmour, K. M., Eliason, E. J., Dressler, T. L., McKenzie, D. J., Bates, A. E., Lawrence, M. J., Fangue, N. et al. (2023). The ecological relevance of critical thermal maxima methodology for fishes. *J. Fish Biol.* **1**, 1-17.

Dulvy, N. K., Fowler, S. L., Musick, J. A., Cavanagh, R. D., Kyne, P. M., Harrison, L. R., Carlson, J. K., Davidson, L. N. K., Fordham, S. V., Francis, M. P. et al. (2014). Extinction risk and conservation of the world's sharks and rays. *Elife* **3**, e00590. doi:10.7554/eLife.00590

Dulvy, N. K., Pacoureau, N., Rigby, C. L., Pollom, R. A., Jabado, R. W., Ebert, D. A., Finucci, B., Pollock, C. M., Cheok, J., Derrick, D. H. et al. (2021). Overfishing drives over one-third of all sharks and rays toward a global extinction crisis. *Curr. Biol.* **31**, 4773-4787.e8. doi:10.1016/j.cub.2021.08.062

Earhart, M. L., Blanchard, T. S., Morrison, P. R., Strowbridge, N., Penman, R. J., Brauner, C. J., Schulte, P. M. and Baker, D. W. (2023). Identification of upper thermal thresholds during development in the endangered Nechako white

sturgeon with management implications for a regulated river. *Conserv. Physiol.* **11**, coad032. doi:10.1093/conphys/coad032

Ebert, D. A., White, W. T., Goldman, K. J., Compagno, L. J. V., Daly-Engel, T. S. and Ward, R. D. (2010). Resurrection and redescription of *Squalus suckleyi* (Girard, 1854) from the North Pacific, with comments on the Squalus acanthias subgroup (Squaliformes: Squalidae). *Zootaxa* **2612**, 22. doi:10.11646/zootaxa.2612.1.2

Ekström, A., Jutfelt, F. and Sandblom, E. (2014). Effects of autonomic blockade on acute thermal tolerance and cardioventilatory performance in rainbow trout, Oncorhynchus mykiss. *J. Therm. Biol.* **44**, 47-54. doi:10.1016/j.jtherbio.2014.06.002

Enders, E. C. and Durhack, T. C. (2022). Metabolic rate and critical thermal maximum CTmax estimates for westslope cutthroat trout, *Oncorhynchus clarkii lewisi*. *Conserv. Physiol.* **10**, coac071. doi:10.1093/conphys/coac071

Ern, R., Norin, T., Gamperl, A. K. and Esbaugh, A. J. (2016). Oxygen dependence of upper thermal limits in fishes. *J. Exp. Biol.* **219**, 3376-3383. doi:10.1242/jeb.143495

Ern, R., Chung, D., Frieder, C. A., Madsen, N. and Speers-Roesch, B. (2020). Oxygen-dependence of upper thermal limits in crustaceans from different thermal habitats. *J. Therm. Biol.* **93**, 102732. doi:10.1016/j.jtherbio.2020.102732

Ern, R., Andreassen, A. H. and Jutfelt, F. (2023). Physiological mechanisms of acute upper thermal tolerance in fish. *Physiology* **38**, 141-158. doi:10.1152/physiol.00027.2022

Fangue, N. A. and Bennett, W. A. (2003). Thermal tolerance responses of laboratory acclimated and seasonally acclimatized Atlantic stingray, *Dasyatis sabina*. *Copeia* **2003**, 315-325. doi:10.1643/0045-8511(2003)003[0315:TTROLA]2.0.CO;2

Firth, B. L., Drake, D. A. R. and Power, M. (2021). Seasonal and environmental effects on upper thermal limits of eastern sand darter (*Ammocrypta pellucida*). *Conserv. Physiol.* **9**, coab057. doi:10.1093/conphys/coab057

Gervais, C. R., Nay, T. J., Renshaw, G., Johansen, J. L., Steffensen, J. F. and Rummer, J. L. (2018). Too hot to handle? Using movement to alleviate effects of elevated temperatures in a benthic elasmobranch, *Hemiscyllium ocellatum*. *Mar. Biol.* **165**, 162. doi:10.1007/s00227-018-3427-7

Gervais, C. R., Huveneers, C., Rummer, J. L. and Brown, C. (2021). Population variation in the thermal response to climate change reveals differing sensitivity in a benthic shark. *Glob. Chang. Biol.* **27**, 108-120. doi:10.1111/gcb.15422

Giacomin, M., Schulte, P. M. and Wood, C. M. (2017). Differential Effects of Temperature on Oxygen Consumption and Branchial Fluxes of Urea, Ammonia, and Water in the Dogfish Shark (*Squalus acanthias suckleyi*). *Physiol. Biochem. Zool.* **90**, 627-637. doi:10.1086/694296

Gilbert, M. J. H., Harris, L. N., Malley, B. K., Schimnowski, A., Moore, J.-S. and Farrell, A. P. (2020). The thermal limits of cardiorespiratory performance in anadromous Arctic char (*Salvelinus alpinus*): a field-based investigation using a remote mobile laboratory. *Conserv. Physiol.* **8**, coaa036. doi:10.1093/conphys/coaa036

Grinder, R. M., Bassar, R. D. and Auer, S. K. (2020). Upper thermal limits are repeatable in Trinidadian guppies. *J. Therm. Biol.* **90**, 102597. doi:10.1016/j.jtherbio.2020.102597

Haverinen, J. and Vornanen, M. (2020). Atrioventricular block, due to reduced ventricular excitability, causes the depression of fish heart rate in fish at critically high temperatures. *J. Exp. Biol.* **223**, jeb.225227. doi:10.1242/jeb.225227

Heath, A. G. and Hughes, G. M. (1973). Cardiovascular and respiratory changes during heat stress in rainbow trout (*Salmo gairdneri*). *J. Exp. Biol.* **59**, 323-338. doi:10.1242/jeb.59.2.323

Hellemans, J., Mortier, G., De Paepe, A., Speleman, F. and Vandesompele, J. (2008). qBase relative quantification framework and software for management and automated analysis of real-time quantitative PCR data. *Genome Biol.* **8**, R19. doi:10.1186/gb-2007-8-2-r19

Illing, B., Downie, A. T., Beghin, M. and Rummer, J. L. (2020). Critical thermal maxima of early life stages of three tropical fishes: Effects of rearing temperature and experimental heating rate. *J. Therm. Biol.* **90**, 102582. doi:10.1016/j.jtherbio.2020.102582

Jeffries, K. M., Connon, R. E., Davis, B. E., Komoroske, L. M., Britton, M. T., Sommer, T., Todgham, A. E. and Fangue, N. A. (2016). Effects of high temperatures on threatened estuarine fishes during periods of extreme drought. *J. Exp. Biol.* **219**, 1705-1716. doi:10.1242/jeb.134528

Jeffries, K. M., Fangue, N. A. and Connon, R. E. (2018). Multiple sub-lethal thresholds for cellular responses to thermal stressors in an estuarine fish. *Comp. Biochem. Physiol. A Mol. Integr. Physiol.* **225**, 33-45. doi:10.1016/j.cbpa.2018.06.020

Joyce, W. and Perry, S. F. (2020). Hypoxia inducible factor-1 α knockout does not impair acute thermal tolerance or heat hardening in zebrafish. *Biol. Lett.* **16**, 20200292. doi:10.1098/rsbl.2020.0292

Jutfelt, F., Roche, D. G., Clark, T. D., Norin, T., Binning, S. A., Speers-Roesch, B., Amcoff, M., Morgan, R., Andreassen, A. H. and Sundin, J. (2019). Brain cooling marginally increases acute upper thermal tolerance in Atlantic cod. *J. Exp. Biol.* **222**, jeb208249. doi:10.1242/jeb.208249

Kochhann, D., Sarmento, C. G., de Oliveira, J. C., Queiroz, H. L., Val, A. L. and Chapman, L. J. (2021). Take time to look at the fish: Behavioral response to acute thermal challenge in two Amazonian cichlids. *J. Exp. Zool. Part A. Ecol. Integr. Physiol.* **335**, 735-744. doi:10.1002/jez.2541

Kolhatkar, A., Robertson, C. E., Thistle, M. E., Kurt Gamperl, A. and Currie, S. (2014). Coordination of chemical (trimethylamine oxide) and molecular (heat shock protein 70) chaperone responses to heat stress in elasmobranch red blood cells. *Physiol. Biochem. Zool.* **87**, 652-662. doi:10.1086/676831

Little, A. G., Loughland, I. and Seebacher, F. (2020). What do warming waters mean for fish physiology and fisheries? *J. Fish Biol.* **97**, 328-340. doi:10.1111/jfb.14402

Lo, M., Shahriari, A., Roa, J. N., Tresguerres, M. and Farrell, A. P. (2021). Differential effects of bicarbonate on severe hypoxia- and hypercapnia-induced cardiac malfunctions in diverse fish species. *J. Comp. Physiol. B* **191**, 113-125. doi:10.1007/s00360-020-01324-y

Lupton, C. E. M. and Bennett, W. A. (2023). Thermal Tolerance of Juvenile New England Chain Catsharks, *Scyliorhinus Retifer* Garman, 1881 (Chondrichthyes, Carcharhiniformes, Scyliorhinidae). *Thalass. An Int. J. Mar. Sci.* **39**, 69-76. doi:10.1007/s41208-022-00514-5

Lutterschmidt, W. I. and Hutchison, V. H. (1997). The critical thermal maximum: History and critique. *Can. J. Zool.* **75**, 1561-1574. doi:10.1139/z97-783

MacMillan, H. A. (2019). Dissecting cause from consequence: a systematic approach to thermal limits. *J. Exp. Biol.* **222**, jeb191593. doi:10.1242/jeb.191593

Maness, J. D. and Hutchison, V. H. (1980). Acute adjustment of thermal tolerance in vertebrate ectotherms following exposure to critical thermal maxima. *J. Therm. Biol.* **5**, 225-233. doi:10.1016/0306-4565(80)90026-1

Martin, T. L. and Huey, R. B. (2008). Why "suboptimal" is optimal: Jensen's inequality and ectotherm thermal preferences. *Am. Nat.* **171**, E102-E118. doi:10.1086/527502

McArley, T. J., Morgenroth, D., Zena, L. A., Ekström, A. T. and Sandblom, E. (2022). Prevalence and mechanisms of environmental hyperoxia-induced thermal tolerance in fishes. *Proc. R. Soc. B Biol. Sci.* **289**, 20220840. doi:10.1098/rspb.2022.0840

McDonnell, L. H. and Chapman, L. J. (2015). At the edge of the thermal window: effects of elevated temperature on the resting metabolism, hypoxia tolerance and upper critical thermal limit of a widespread African cichlid. *Conserv. Physiol.* **3**, cov050. doi:10.1093/conphys/cov050

McDonnell, L. H., Reemeyer, J. E. and Chapman, L. J. (2019). Independent and interactive effects of long-term exposure to hypoxia and elevated water temperature on behavior and thermal tolerance of an equatorial cichlid. *Physiol. Biochem. Zool.* **92**, 253-265. doi:10.1086/702712

McDonnell, L. H., Mandrak, N. E., Kaur, S. and Chapman, L. J. (2021). Effects of acclimation to elevated water temperature and hypoxia on thermal tolerance of the threatened pugnose shiner (*Notropis anogenus*). *Can. J. Fish. Aquat. Sci.* **78**, 1257-1267. doi:10.1139/cjfas-2020-0362

Milligan, C. L. and Girard, S. S. (1993). Lactate metabolism in rainbow trout. *J. Exp. Biol.* **180**, 175-193. doi:10.1242/jeb.180.1.175

Morgan, R., Finnøen, M. H. and Jutfelt, F. (2018). CTmax is repeatable and doesn't reduce growth in zebrafish. *Sci. Rep.* **8**, 7099. doi:10.1038/s41598-018-25593-4

Morrison, S. M., Mackey, T. E., Durhack, T., Jeffrey, J. D., Wiens, L. M., Mochnacz, N. J., Hasler, C. T., Enders, E. C., Treberg, J. R. and Jeffries, K. M. (2020). Sub-lethal temperature thresholds indicate acclimation and physiological limits in brook trout *Salvelinus fontinalis*. *J. Fish Biol.* **97**, 583-587. doi:10.1111/jfb.14411

Murchie, K. J., Cooke, S. J., Danylchuk, A. J., Danylchuk, S. E., Goldberg, T. L., Suski, C. D. and Philipp, D. P. (2011). Thermal biology of bonefish (*Albula vulpes*) in Bahamian coastal waters and tidal creeks: An integrated laboratory and field study. *J. Therm. Biol.* **36**, 38-48. doi:10.1016/j.jtherbio.2010.10.005

Nati, J. J. H., Blasco, F. R., Rodde, C., Vergnet, A., Allal, F., Vandeputte, M. and McKenzie, D. J. (2023). In a marine teleost, the significance of oxygen supply for acute thermal tolerance depends upon the context and the endpoint used. *J. Exp. Biol.* **226**, jeb245210. doi:10.1242/jeb.245210

Nawata, C. M., Walsh, P. J. and Wood, C. M. (2015). Physiological and molecular responses of the spiny dogfish shark (*Squalus acanthias*) to high environmental ammonia: scavenging for nitrogen. *J. Exp. Biol.* **218**, 238-248. doi:10.1242/jeb.114967

Nay, T. J., Longbottom, R. J., Gervais, C. R., Johansen, J. L., Steffensen, J. F., Rummer, J. L. and Hoey, A. S. (2021). Regulate or tolerate: Thermal strategy of a coral reef flat resident, the epaulette shark, *Hemiscyllium ocellatum*. *J. Fish Biol.* **98**, 723-732. doi:10.1111/jfb.14616

O'Brien, K. M., Rix, A. S., Egginton, S., Farrell, A. P., Crockett, E. L., Schlauch, K., Woolsey, R., Hoffman, M. and Merriman, S. (2018). Cardiac mitochondrial metabolism may contribute to differences in thermal tolerance of red- and white-blooded Antarctic notothenioid fishes. *J. Exp. Biol.* **221**, jeb177816. doi:10.1242/jeb.177816

O'Brien, K. M., Rix, A. S., Grove, T. J., Sarrimanolis, J., Brooking, A., Roberts, M. and Crockett, E. L. (2020). Characterization of the hypoxia-inducible factor-1 pathway in hearts of Antarctic notothenioid fishes. *Comp. Biochem. Physiol. B Biochem. Mol. Biol.* **250**, 110505. doi:10.1016/j.cbpb.2020.110505

Opdyke, D. F. and Opdyke, N. E. (1971). Splenic responses to stimulation in *Squalus acanthias*. *Am. J. Physiol.* **221**, 623-625. doi:10.1152/ajplegacy.1971.221.2.623

Payne, N. L., Morley, S. A., Halsey, L. G., Smith, J. A., Stuart-Smith, R., Waldock, C. and Bates, A. E. (2021). Fish heating tolerance scales similarly across individual physiology and populations. *Commun. Biol.* **4**, 264. doi:10.1038/s42003-021-01773-3

Potts, L. B., Mandrak, N. E. and Chapman, L. J. (2021). Coping with climate change: Phenotypic plasticity in an imperilled freshwater fish in response to elevated water temperature. *Aquat. Conserv. Mar. Freshw. Ecosyst.* **31**, 2726-2736. doi:10.1002/aqc.3620

Sandblom, E., Cox, G. K., Perry, S. F. and Farrell, A. P. (2009). The role of venous capacitance, circulating catecholamines, and heart rate in the hemodynamic response to increased temperature and hypoxia in the dogfish. *Am. J. Physiol. Integr. Comp. Physiol.* **296**, R1547-R1556. doi:10.1152/ajpregu.90961.2008

Sandrelli, R. M. and Gamperl, A. K. (2023). The upper temperature and hypoxia limits of atlantic salmon (*Salmo salar*) depend greatly on the method utilized. *J. Exp. Biol.* **226**, jeb246227. doi:10.1242/jeb.246227

Schoen, A. N., Treberg, J. R., Wheaton, C. J., Mylniczenko, N. and Gary Anderson, W. (2021). Energy and corticosteroid mobilization following an induced stress response in an elasmobranch fish, the North Pacific spiny dogfish (*Squalus acanthias suckleyi*). *Gen. Comp. Endocrinol.* **310**, 113799. doi:10.1016/j.ygcen.2021.113799

Schulte, P. M., Healy, T. M. and Fangue, N. A. (2011). Thermal performance curves, phenotypic plasticity, and the time scales of temperature exposure. *Integr. Comp. Biol.* **51**, 691-702. doi:10.1093/icb/icr097

Schwieterman, G. D., Rummer, J. L., Bouyoucos, I. A., Bushnell, P. G. and Brill, R. W. (2021a). A lack of red blood cell swelling in five elasmobranch fishes following air exposure and exhaustive exercise. *Comp. Biochem. Physiol. A Mol. Integr. Physiol.* **258**, 110978. doi:10.1016/j.cbpa.2021.110978

Schwieterman, G. D., Winchester, M. M., Shiels, H. A., Bushnell, P. G., Bernal, D., Marshall, H. M. and Brill, R. W. (2021b). The effects of elevated potassium, acidosis, reduced oxygen levels, and temperature on the functional properties of isolated myocardium from three elasmobranch fishes: clearnose skate (*Rostroraja eglanteria*), smooth dogfish (*Mustelus canis*). *J. Comp. Physiol. B* **191**, 127-141. doi:10.1007/s00360-020-01328-8

Treberg, J. R. and Driedzic, W. R. (2006). Maintenance and accumulation of trimethylamine oxide by winter skate (*Leucoraja ocellata*): Reliance on low whole animal losses rather than synthesis. *Am. J. Physiol. Regul. Integr. Comp. Physiol.* **291**, 1790-1798. doi:10.1152/ajpregu.00150.2006

Treberg, J. R., Martin, R. A. and Driedzic, W. R. (2003). Muscle enzyme activities in a deep-sea squaloid shark, *Centroscyllium fabricii*, compared with its shallow-living relative, squalus acanthias. *J. Exp. Zool. Part A Comp. Exp. Biol.* **300**, 133-139. doi:10.1002/jez.a.10318

Tribuzio, C. A. and Kruse, G. H. (2012). Life history characteristics of a lightly exploited stock of *Squalus suckleyi*. *J. Fish Biol.* **80**, 1159-1180. doi:10.1111/j.1095-8649.2012.03241.x

Turko, A. J., Nolan, C. B., Balshine, S., Scott, G. R. and Pitcher, T. E. (2020). Thermal tolerance depends on season, age and body condition in imperilled redside dace *Clinostomus elongatus*. *Conserv. Physiol.* **8**, coaa062. doi:10.1093/conphys/coaa062

Vandesompele, J., De Preter, K., Pattyn, F., Poppe, B., Van Roy, N., De Paepe, A. and Speleman, F. (2002). Accurate normalization of real-time quantitative RT-PCR data by geometric averaging of multiple internal control genes. *Genome Biol.* **3**, RESEARCH0034. doi:10.1186/gb-2002-3-7-research0034

Villalobos, A. R. A. and Renfro, J. L. (2007). Trimethylamine oxide suppresses stress-induced alteration of organic anion transport in choroid plexus. *J. Exp. Biol.* **210**, 541-552. doi:10.1242/jeb.02681

Watanabe, Y. Y. and Payne, N. L. (2023). Thermal sensitivity of metabolic rate mirrors biogeographic differences between teleosts and elasmobranchs. *Nat. Commun.* **14**, 2054. doi:10.1038/s41467-023-37637-z

Wells, Z. R. R., McDonnell, L. H., Chapman, L. J. and Fraser, D. J. (2016). Limited variability in upper thermal tolerance among pure and hybrid populations of a cold-water fish. *Conserv. Physiol.* **4**, cow63. doi:10.1093/conphys/cow063

Wheeler, C. R., Lang, B. J., Mandelman, J. W. and Rummer, J. L. (2022). The upper thermal limit of epaulette sharks (*Hemiscyllium ocellatum*) is conserved across three life history stages, sex and body size. *Conserv. Physiol.* **10**, coac074. doi:10.1093/conphys/coac074

Yeager, D. P. and Ultsch, G. R. (1989). Physiological regulation and conformation: a BASIC program for the determination of critical points. *Physiol. Zool.* **62**, 888-907. doi:10.1086/physzool.62.4.30157935

Zhang, Y. and Kieffer, J. D. (2014). Critical thermal maximum (CTmax) and hematology of shortnose sturgeons (*Acipenser brevirostrum*) acclimated to three temperatures. *Can. J. Zool.* **92**, 215-221. doi:10.1139/cjz-2013-0223

Zimmer, A. M. and Wood, C. M. (2014). Exposure to acute severe hypoxia leads to increased urea loss and disruptions in acid-base and ionoregulatory balance in dogfish sharks (*Squalus acanthias*). *Physiol. Biochem. Zool.* **87**, 623-639. doi:10.1086/677884